Thermochimica Acta, 207 (1992) 147–159
Elsevier Science Publishers B.V., Amsterdam

An investigation of the thermal decomposition of poly(3-nitratomethyl-3-methyloxetane)

P.F. Bunyan

Defence Research Agency, Royal Armament Research and Development Establishment, Fort Halstead, Sevenoaks, Kent TN14 7BP (UK)

(Received 20 December 1991)

Abstract

The decomposition of poly(3-nitratomethyl-3-methyloxetane) (polyNIMMO) was studied using the techniques of differential calorimetry, thermogravimetry, heat flow calorimetry and adiabatic calorimetry. In all cases the decomposition appears to follow an Arrhenius temperature dependence relationship and a single non-autocatalytic first-order rate law throughout the reaction. This contrasts with the autocatalytic decomposition behaviour of traditional nitrate ester propellant ingredients, at present in service use.

INTRODUCTION

Until recently, composite propellants have generally consisted of an inorganic oxidant (typically ammonium perchlorate) dispersed in a polymeric binder such as polybutadiene. In addition the polymer acts as a fuel and also provides this class of propellants with many desirable physical properties. Higher performance can be achieved by including a large proportion of a high energy explosive material such as the nitramine RDX (1,3,5-trinitro-1,3,5-triaza-cyclohexane). However, the hard and brittle nature of this substance means that the main advantage of composite propellants, good mechanical properties, is diminished.

The use of a rubbery binder which is itself energetic would allow the use of a lower proportion of solids to yield the required performance, while restoring the desirable mechanical properties. In addition, a reduction in the proportion of RDX should lead to lower vulnerability. One promising material to fulfil this role, poly(3-nitratomethyl-3-methyloxetane) (polyNIMMO), has been developed at RARDE [1].

PolyNIMMO possesses polyether linkages in the polymer backbone and pendent nitrate ester groups, both of which are potentially chemically

Correspondence to: P.F. Bunyan, Defence Research Agency, Royal Armament Research and Development Establishment, Fort Halstead, Sevenoaks, Kent TN14 7BP, UK.

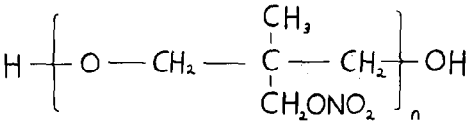

Fig. 1. Structure of polyNIMMO.

labile (Fig. 1). It is therefore important to understand the ageing mechanism of this material to allow the development of propellants with acceptable service lives.

Some experiments to determine the thermal decomposition of polyNIMMO over a range of different conditions using a variety of thermoanalytical techniques are described here.

EQUIPMENT AND MATERIALS

Differential calorimetry and thermogravimetry

A Mettler TG50 thermobalance was used to record rising temperature mass loss curves. Temperature calibration by the recommended Curie point transition method was found to be inaccurate when the thermobalance was operated isothermally; the temperature was therefore measured directly with a thermocouple. Samples were contained in 70 μl alumina crucibles (Mettler part no. ME 24123).

Differential calorimetry was performed in a Mettler DSC-20 measuring cell. Samples were contained in 40 μl aluminium pans (Mettler part no. ME 27331) covered by a lid perforated with a single pinhole.

Heat flow calorimetry

A Thermometric type 2277 microcalorimeter ("Thermal Activity Monitor") was used to monitor heat flow. Samples of polyNIMMO (3.6 ± 0.1 g) were sealed in 3 cm^3 glass ampoules (Thermometric part no. 2277-303).

Adiabatic calorimetry

An accelerating rate calorimeter (ARC) manufactured by Columbia Scientific Industries of Austin, TX, was used. Samples were contained in 1 in diameter spherical titanium bombs (CSI part no. 851-3068). Sample bombs were cleaned before use by heating to 600°C in an oven while purging the inside of the bomb with oxygen to remove carbonaceous deposits.

Data were recorded and processed using the CSI-ARC software package Version 1.2, running on a Hewlett-Packard ES/12 Vectra microcomputer.

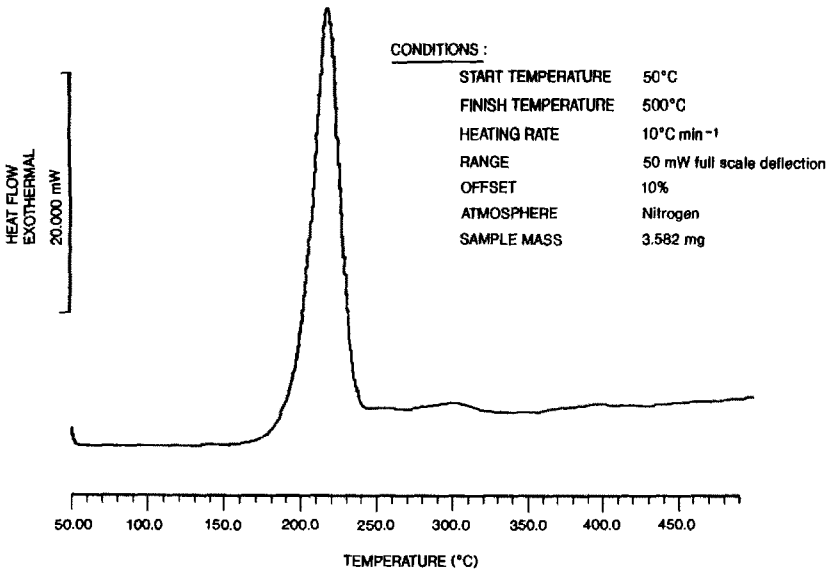

Fig. 2. DSC trace of polyNIMMO.

Sample

PolyNIMMO batch no. 1.38 synthesized at RARDE, Waltham Abbey, UK, in January 1990, was used throughout this work,.

EXPERIMENTAL AND RESULTS

Differential calorimetry and thermogravimetry

Differential scanning calorimetry (DSC) revealed a large exothermic peak from 150 to 240°C. This is a typical feature found in nitrate-ester-based propellants. There is little evidence of exothermic reactions occurring above this temperature (Fig. 2).

Scanning thermogravimetric analysis (TGA) showed a mass loss step, accounting for around 2/3 of the starting mass, from 150 to 240°C corresponding to the DSC exotherm. Almost all of the remaining sample mass was lost gradually from 250 to 500° (Fig. 3).

Isothermal decomposition curves recorded at 180°C, both by differential calorimetry and TGA, exhibited a first-order decay rate law throughout the entire decomposition. This can be seen from the straight line first-order plots shown in Figs. 4 and 5.

A series of isothermal decomposition curves were recorded by differential calorimetry between 180 and 215°C (Table 1). The temperature dependence of the reaction could then be found from a plot of ln k vs.

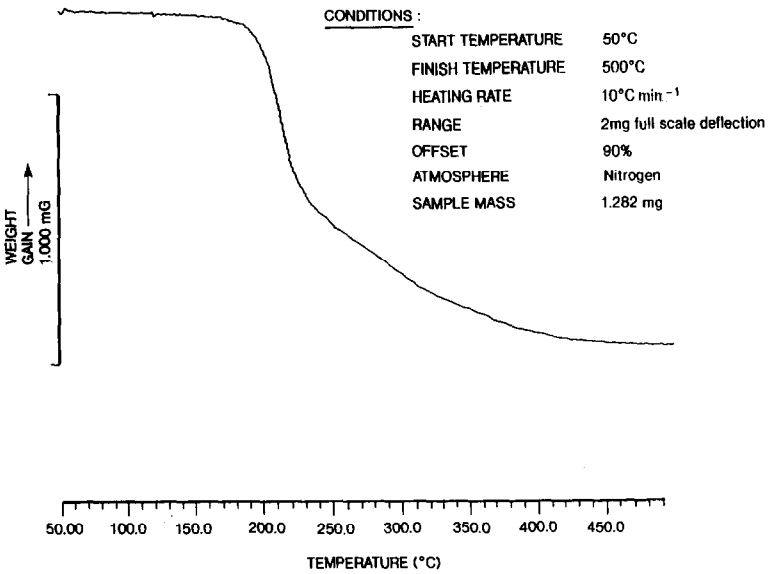

Fig. 3. TGA trace of polyNIMMO.

$1/T$ where k is the rate constant and T is the absolute temperature (Fig. 6). This procedure has been described in detail by Beckmann et al. [2].

The deduced constants in the Arrhenius equation were tested by a series of half-life ageing experiments at lower temperatures as recommended in ref. 3 (Table 2).

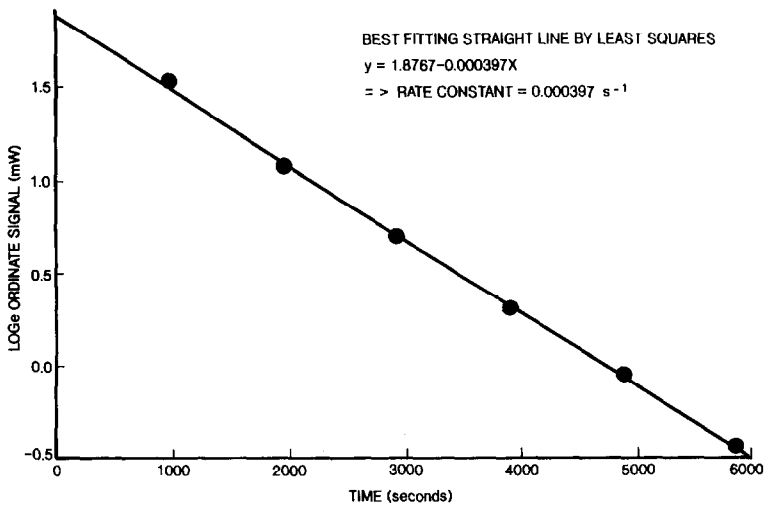

Fig. 4. First-order rate law plot for thermal decomposition, by isothermal calorimetry at 180°C.

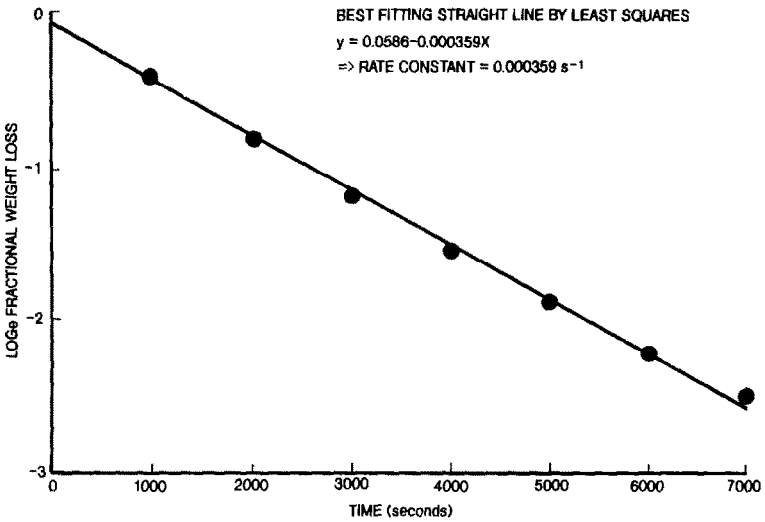

Fig. 5. First-order rate law plot for thermal decomposition, by isothermal thermogravimetry at 180°C.

Heat flow calorimetry (HFC)

In view of the influence of the free volume atmosphere on the decomposition of nitrate-ester-based propellants found in the past [4], experiments were conducted both on untreated samples (i.e. samples simply sealed with air) and also on samples where dissolved air had been removed by storage under vacuum and the free volume space packed with nitrogen before sealing. Heat generation was recorded for a range of temperatures and used to plot Arrhenius curves for both the anaerobic and aerobic decomposition of polyNIMMO (Figs. 7 and 8). Activation energies were deduced for

TABLE 1

Isothermal differential calorimetry [a]

Temperature (K)	Decay rate constant (s^{-1})	Reaction order
453.15	0.000439	0.94
458.15	0.000643	0.98
463.15	0.001049	0.99
468.15	0.001695	0.99
473.15	0.002658	1.06
478.15	0.003849	1.01
483.15	0.006036	1.00
488.15	0.009952	0.97

[a] From plot of ln k vs. $1/T$ (Fig. 6) the activation energy is 163.67 kJ mol^{-1}, and the pre-exponential factor is 3.065×10^{15} s^{-1}.

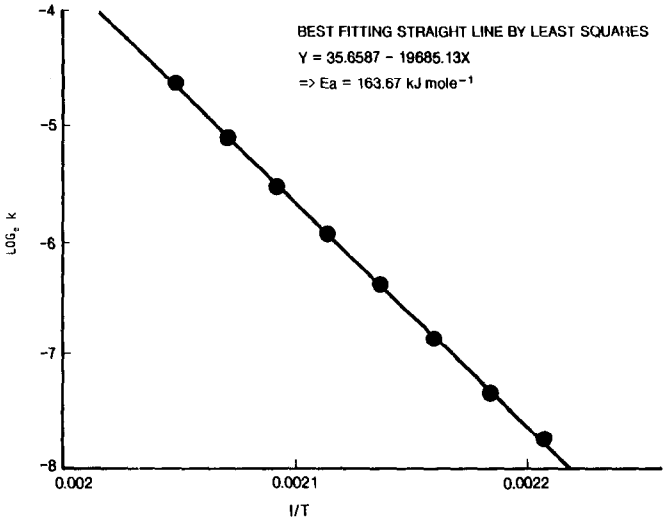

Fig. 6. Arrhenius plot of thermal decomposition, using isothermal calorimetry data.

the reaction at the point where 0.5, 1.0, 1.5 and 2.0 J g^{-1} of heat had been evolved using the procedure described in ref. 4 (Table 3).

In order to check that the difference in heat generation seen when oxygen was excluded was caused by the absence of oxygen and not by some artefact of the degassing procedure (e.g. the removal of an unstable, volatile, minor component under vacuum) some ampoules of polyNIMMO were packed with oxygen instead of nitrogen before sealing. Heat generation rates monitored over the first 50 h of storage at 91.4°C for samples packed with nitrogen, air and oxygen are shown in Fig. 9 and these clearly show that the effect is due to the progressive influence of oxygen.

Adiabatic calorimetry

ARC runs were initially performed on samples small enough to allow the calorimeter to maintain adiabatic conditions (runs nos. 162 and 163). Data were plotted and interpreted by applying the theoretical principles de-

TABLE 2

Validation of kinetic constants found by differential calorimetry

Temperature (K)	Predicted half life (min)	Observed fractional decrease in energy after ageing (%)
443.15	83	42.7
433.15	205	37.25
418.15	1050	39.5

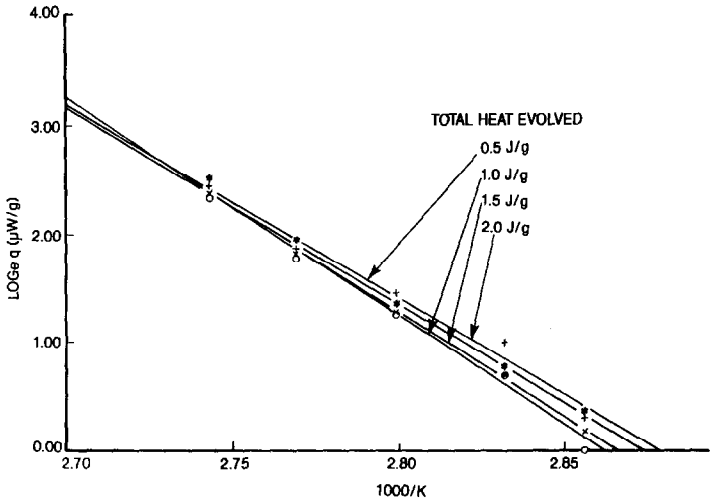

Fig. 7. Temperature dependence of polyNIMMO decomposition (with nitrogen). Total heat evolved: +, 0.5 J g^{-1}; ○, 1.0 J g^{-1}; ×, 1.5 J g^{-1}; *, 2.0 J g^{-1}.

scribed by Townsend and Tou [5]. The result of a typical decomposition, showing the self-heat rate as a function of $1/T$ is shown in Fig. 10. This indicates that the decomposition occurs smoothly and as a single reaction. A plot of pseudo rate constant K^* vs. $1/T$ showed a linear relationship when $n = 1$, indicating that the reaction follows a first-order non-autocatalytic rate law (Fig. 11).

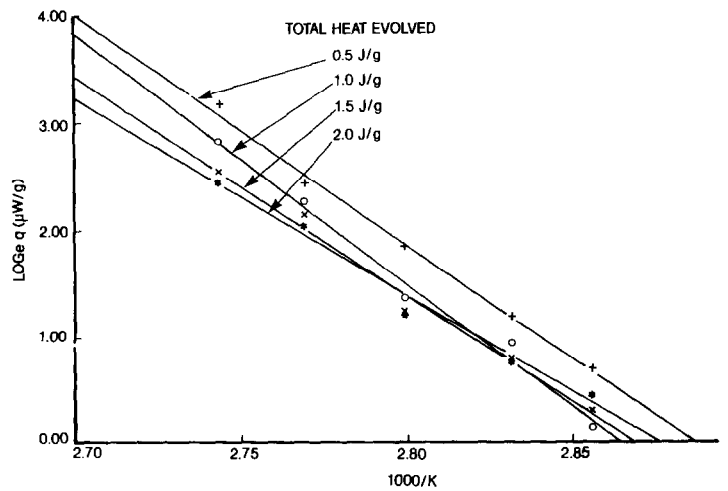

Fig. 8. Temperature dependence of polyNIMMO decomposition (with air). Total heat evolved: +, 0.5 J g^{-1}; ○, 1.0 J g^{-1}; ×, J g^{-1}; *, 2.0 J g^{-1}.

TABLE 3

Heat flow calorimetry

Total heat evolution ($J\ g^{-1}$)	Atmosphere	Temperature (°C)	Heat generation rate ($\mu W\ g^{-1}$)	Activation energy ($kJ\ mol^{-1}$)	R [a]
2.0	Nitrogen	91.4	11.014		
		88.0	6.714		
		84.1	3.838	151	−0.9997
		80.0	2.128		
		77.0	1.427		
1.5	Nitrogen	91.4	10.782		
		88.0	6.413		
		84.1	3.644	161	−0.9994
		80.0	2.039		
		77.0	1.174		
1.0	Nitrogen	91.4	10.767		
		88.0	6.201		
		84.1	3.653	167	−0.9954
		80.0	2.099		
		77.0	1.019		
0.5	Nitrogen	91.4	11.597		
		88.0	6.464		
		84.1	4.302	148	−0.9910
		80.0	2.719		
		77.0	1.347		
2.0	Air	91.4	11.590		
		88.0	7.723		
		84.1	3.573	152	−0.9945
		80.0	2.201		
		77.0	1.553		
1.5	Air	91.4	12.497		
		88.0	8.505		
		84.1	3.531	169	−0.9945
		80.0	2.223		
		77.0	1.300		
1.0	Air	91.4	16.891		
		88.0	9.629		
		84.1	3.929	193	−0.9937
		80.0	2.543		
		77.0	1.145		
0.5	Air	91.4	23.685		
		88.0	11.513		
		84.1	6.408	177	−0.9979
		80.0	3.343		
		77.0	2.017		

[a] R, correlation between ln q and $1000/K$ (Figs. 7 and 8).

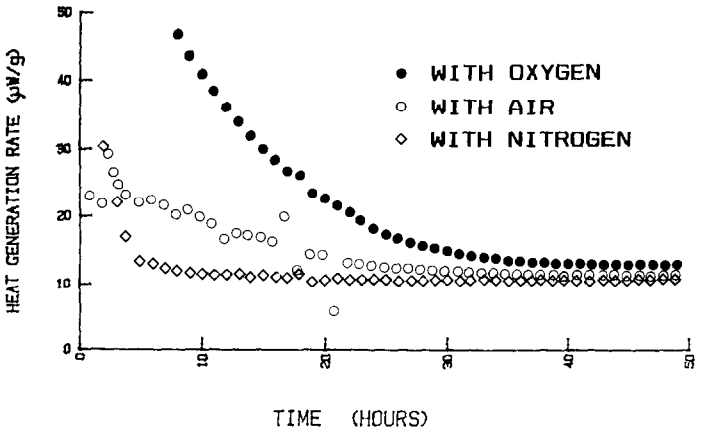

Fig. 9. Heat generation at 91.4°C (packed with different atmospheres).

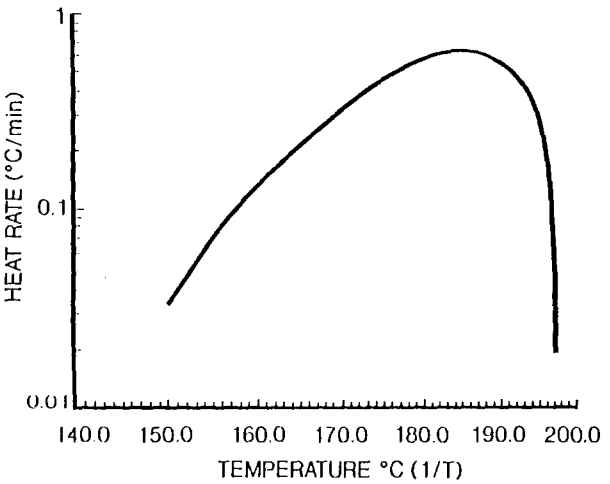

Fig. 10. Plot of ARC self-heat rate as a function of $1/T$ for polyNIMMO.

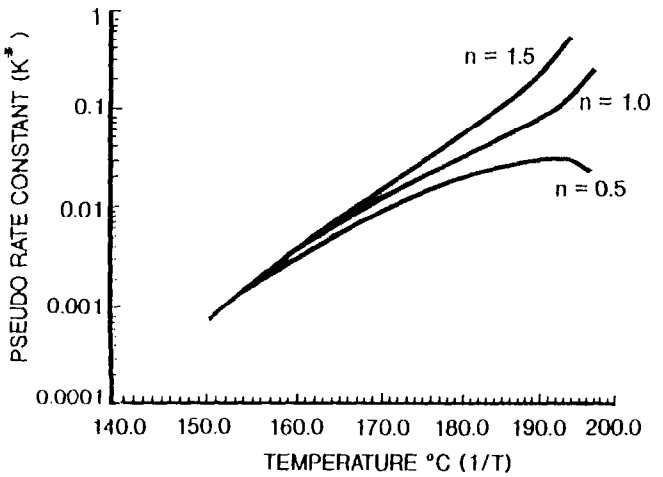

Fig. 11. Plot of ARC log k^* as a function of $1/T$ for polyNIMMO.

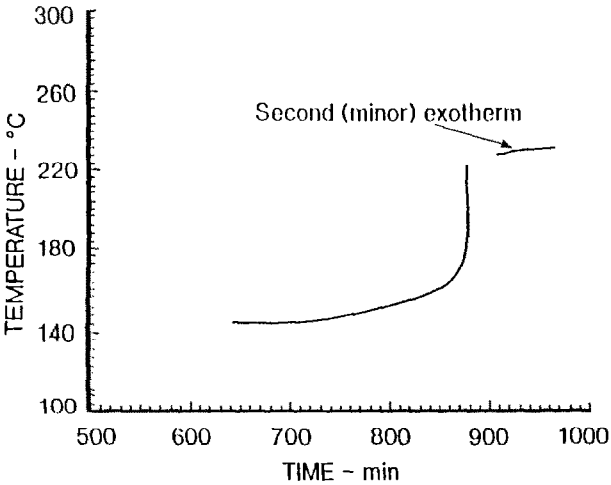

Fig. 12. Plot of ARC temperature vs. time for larger sample of polyNIMMO.

The use of larger samples to improve precision (run nos. 153 and 156) resulted in loss of temperature control during the main exotherm. However, this procedure did reveal the existence of a second, minor exotherm above 200°C (Fig. 12).

TABLE 4

Summary of polyNIMMO ARC runs

Run Parameter [a]	Run no.					
	162	163	153	156	160	161
Sample mass (g)	0.176	0.187	0.298	0.283	0.206	0.208
ϕ	15.09	14.18	9.26	9.74	12.97	12.89
T_0 (°C)	150.4	147.5	143.2	146.5	140.4	147.6
T_{mr}(sys) (°C)	184.5	190.6	185.5	186.2	178.5	181.7
P_{mr}(sys) (lbf in^{-2})	121.8	139.6	230.1	282.3	[b]	[b]
t_{mr}(sys) (min)	207.6	208.4	234.9	155.3	218.6	208.4
dT_{ab}(sys) (°C)	46.63	59.42	[c]	[c]	43.3	59.42
dT_{ab} (°C)	703.5	842.6	[c]	[c]	561.6	646.7
t_{mr} (min)	13.76	14.70	[c]	[c]	16.85	25.93
Heat of reaction (J g^{-1})	1473	1763	[c]	[c]	1175	1353
Activation energy (kJ mol^{-1})	172.6	178.6	[c]	[c]	184.2	185.4
ln A (s^{-1})	38.06	39.88	[c]	[c]	41.36	41.71

[a] T_0, temperature at which exotherm is first detected; ϕ, thermal inertia; T_{mr}, temperature of maximum self-heating rate; P_{mr}, pressure at maximum self-heating rate; t_{mr}, time to maximum rate after exotherm first detected; A, pre-exponential factor. The suffix (sys) indicates the entire system comprising the combination of sample and ARC sample bomb.

[b] No pressure rise as the bomb was open to the atmosphere.

[c] Temperature control lost during exotherm, therefore data not quantitative.

To allow closer comparison between ARC results and those from isothermal calorimetry, some isobaric experiments were conducted by disconnecting the pressure transducer line from the bomb at the start of the run so that enthalpy rather than internal energy was used to estimate the degree of advancement of the reaction (run nos. 160 and 162). The results of ARC experiments are summarized in Table 4.

DISCUSSION

A good fit to an Arrhenius temperature dependence law is indicated by the straight line plot obtained from differential calorimetry data (Fig. 6). The deduced activation energy (164.7 kJ mol^{-1}) is within the range associated with reaction mechanisms controlled by the cleavage of nitrate ester bonds. The Arrhenius curve drawn using HFC data obtained at far lower temperatures gives comparable values for activation energy (Table 3), suggesting that this decomposition mechanism is dominant over a wide temperature range.

Differences in the HFC results caused by altering the surrounding atmosphere (Fig. 9) would suggest that the availability of oxygen will be an important consideration when predicting the ageing characteristics of this material.

The ARC results are in agreement with the other approaches as far as indicating a simple, single mechanism over a wide temperature range and throughout the reaction. The higher value given for the heat of reaction (internal energy) measured in the sealed bomb experiments than for the heat of reaction (enthalpy) measured in the open bomb experiments would be expected for a gas-generating reaction.

Slightly higher values for the activation energy are indicated in the ARC runs than given by either of the isothermal techniques. A lack of agreement between the absolute values obtained for kinetic parameters determined using isothermal and rising temperature methods has been reported in the past [6–9].

The half-life prediction tests (Table 2) suggest that this material survives storage at lower temperatures better than predicted from the higher temperature experiments, although the error is fairly constant at all temperatures studied. If this discrepancy were due to an underestimate of activation energy, it would be expected to get progressively larger with extrapolation. An alternative explanation would be the presence of a second, exothermic reaction occurring at a higher temperature than the principal one, which is always included in the enthalpy measurement by DSC, but is unaffected by storage at lower temperatures. Evidence for the existence of such an exotherm is provided by the ARC runs on oversize samples (Fig. 12).

The fact that the observed reaction mechanism is so simple is worth commenting upon. Most traditional nitrate-ester-based explosive ingredients, such as nitrocellulose and nitroglycerine, show complex kinetic behaviour due to autocatalysis and competing reactions as the decomposition proceeds, particularly when a stabilizer is not present, and are influenced significantly by storage conditions [10–13]. A relatively simple decomposition behaviour of polyNIMMO has also been reported recently by Chen and Brill using the technique of scanning TGA [14]. They speculate that this may be due to the ease with which NO_x could diffuse away from the reacting mass, the comparatively low oxygen balance of polyNIMMO, or the absence of secondary nitrate groups. A further hypothesis which would also be consistent with these observations would be that the polymer backbone itself has a strong affinity for the highly reactive initial products of nitrate ester bond breakage leading to chemically benign products. Supporting evidence for this may be found in ref. 15, which reports that the thermolysis of the nitrate ester groups and chain scission are correlated and presumably interrelated. It is also reported that both of these processes are significantly retarded when the traditional nitrate ester stabilizer, 2-nitrodiphenylamine, is added to the system.

CONCLUSIONS

The rate of slow thermal decomposition of polyNIMMO at temperatures below 220°C can be described well by an Arrhenius equation. Values deduced for the activation energy suggest a reaction mechanism governed by nitrate ester bond breakage.

The reaction appeared to follow a first-order decay rate law throughout the entire decomposition. No evidence of autocatalytic behaviour was seen. This is surprisingly simple behaviour for an unstabilized nitrate ester propellant material and may indicate that polyNIMMO possesses some intramolecular chemical stabilization capability.

The decomposition mechanism can be influenced by the availability of oxygen.

REFERENCES

1 A.W. Arber, G.E. Bagg, M.E. Colclough, H. Desai, R.W. Millar, N.C. Paul, D.A. Salter and M.J. Stewart, 21st Int. Conf. of ICT, Technology of Polymer Compounds and Energetic Materials, Karlsruhe, FRG, 3–6 July 1990, Paper V3.
2 J.W. Beckmann, J.S. Wilkes and R.R. McGuire, Thermochim. Acta, 19 (1977) 111.
3 Arrhenius Kinetic Constants for Thermally Unstable Materials, ANSI/ASTM, E698, 1979.
4 P.F. Bunyan, RARDE Memorandum 43/86, HMSO, London, 1987.
5 D.I. Townsend and J.C. Tou, Thermochim. Acta, 37 (1980) 1.
6 P.P. Lee and M.H. Back, Thermochim. Acta, 127 (1988) 89.

7 R.K. Agrawal, J. Therm. Anal., 31 (1986) 1253.
8 M. Maciejewski and A. Reller, Thermochim. Acta, 110 (1987) 145.
9 P.D. Garn, Thermochim. Acta, 110 (1987) 141.
10 C.E. Waring and G. Krastins, J. Phys. Chem., 74 (1970) 999.
11 L. Phillips, Ph.D. Thesis, University of London, June 1949.
12 R.W. Phillips, C.A. Orlick and R. Steinberger, J. Phys. Chem., 59 (1955) 1034.
13 L. Dauerman and Y.A. Tajima, AIAA J., 6(8) (1968) 1468.
14 J.K. Chen and T.B. Brill, Thermochim. Acta, 181 (1991) 71.
15 P.F. Bunyan, A.V. Cunliffe and A. Davis, Proc. 16th Int. Pyrotechnics Seminar, Jonkoping, Sweden, 24–28 June 1991, p. 131.